NJC

ROYAL SOCIETY OF CHEMISTRY

PAPER

View Article Online
View Journal | View Issue

Cite this: *New J. Chem.*, 2024, **48**, 15577

Synthesis of a tube-like tetra-bipyridyl, tetra-ethylacetato-calix[4]arene in 1,3-alternate conformation and the unexpected crystal structure of its [bpy($CoCl_2$)]$_3$-[bpy($CoCl_2$)(H_2O)] complex†

Maxime Mourer,[a] Younes Bouizi,[c] Sébastien Leclerc,[d] Bernard Malaman[b] and Jean-Bernard Regnouf de Vains *[a]

Received 29th May 2024,
Accepted 24th July 2024

DOI: 10.1039/d4nj02476a

rsc.li/njc

Treating conic tetra-*para*-ethylacetato-calix[4]arene (**1**) with 2.2 equivalents of K_2CO_3 and 4 equivalents of 6-bromomethyl-6′-methyl-2,2′-bipyridine affords the expected fully substituted podand, mainly in its 1,3-alternate conformation (**2**). This tube-like bipyridyl derivative **2** was subjected to complexation studies with $CoCl_2{\cdot}6H_2O$ to give a blue tetra cobalt(II) complex species (**3**). This complex displays a unique group of 6 aromatic bipyridyl ^{1}H-NMR resonance signals demonstrating its high symmetry, while X-ray diffraction studies showed the presence of 3 expected tetrahedral bpy($CoCl_2$) units and 1 original trigonal bipyramidal unit involving the adjunction of a fifth ligand assumed to be H_2O that could participate in the crystal scaffold.

Introduction

Calixarene platforms offer a wide range of structural and functional modulations[1–6] and are the subject of intense investigations, particularly for the building of highly organized metal chelators, with objectives of separation, purification, waste depollution, enzyme mimicry or detection.[7–19]

Our previous contribution to the field focused on the building of calixarene-based chelators based mainly on 2,2′-bipyridine complexing units, whose number and arrangement along the calix[4]arene axis generate a coordinating environment that is prone to forming complexes with metal ions *via* their preferred coordination geometry with high selectivity.[20–34]

We reported a recent and representative example that showed the feasibility of $L_2Cu(I)_4$ coordination with two shared Cu(I)(bipyridine)$_2$ subunits assembling two conic conformers of the tetra-*O*-2,2′-bipyridyl derivative of tetra-*para*-*tert*-butyl-calix[4]arene.[35]

In order to widen the scope of such metal ion-based spatial organizing behavior to complexation in water or at the air–water interface, we designed the analogous conic ligand bearing, in place of *tert*-butyl groups, *para*-ethylacetate ones which are prone to generate water-solubility and/or amphiphilicity after hydrolysis.

Surprisingly, the tetra-ethylacetato ligand (**2**) thus obtained does not satisfy the structural/conformational requirements, *i.e.* the conic conformation of the calixarene core, instead it gives a 1,3-alternate tetrasubstituted analogue. This particular structure was found highly interesting for the building of new types of polynuclear complexes and coordination polymers. Various metal ions have thus been tested. Among these, cobalt(II) chloride gave blue monocrystals that were suitable for X-ray diffraction analysis.

We report here the synthesis of the new ligand **2**, its complexation study with $CoCl_2{\cdot}6H_2O$, and the characterization of the resulting complex.

The studies were carried out through complex formation survey using UV-visible spectroscopy titration, complex structure analysis in solution using ESI-MS and, even if paramagnetic, ^{1}H- and ^{13}C-NMR spectroscopy. We also studied the complex in the solid state through FTIR spectrometry, elemental analysis and X-ray diffraction. The (6,6′-dimethyl-2,2′-bipyridyl)Co(Cl)$_2$ complex (**4**) was prepared in parallel for comparative studies.[36]

Results and discussion

Synthesis

Tetra ethyl ester **1**[37] and 6-bromomethyl-6′-methyl-2,2′-bipyridine[38] were synthesized according to the literature.

In a one-pot process that should involve the participation of ester groups in the complexation/chelation of K^+ ions, the

[a] *L2CM, UMR 7053 CNRS, Université de Lorraine, France. E-mail: jean-bernard.regnouf@univ-lorraine.fr*
[b] *IJL, UMR 7498, Université de Lorraine, France*
[c] *CRM2, UMR 7036 CNRS, Université de Lorraine, France*
[d] *LEMTA, UMR 7563 CNRS, Université de Lorraine, France*

† Electronic supplementary information (ESI) available. CCDC 2357976. For ESI and crystallographic data in CIF or other electronic format see DOI: https://doi.org/10.1039/d4nj02476a

reaction was performed in refluxing MeCN with 2.2 equiv. of K_2CO_3 on calixarene **1**, *i.e.* 4.4 basic units *vs.* 4 OH groups, followed by the reaction of 4.1 equivalents of 6-bromomethyl-6′-methyl-2,2′-bipyridine, affording the tetra-substituted podand (**2**). Surprisingly, **2** is formed in the 1,3-alternate conformation and isolated with a global yield of 40% (formal 90% yield *via* alkylation) after careful purification (Scheme 1). Such preferential alternate conformation was also observed with tetra-[4-cyanomethyl]-calix[4]arene in similar conditions.[39,40]

The tetra cobalt(II) complex **3** was prepared by reaction of a solution of ligand **2** in CH_2Cl_2 with a solution of 4 equivalents of $CoCl_2{\cdot}6H_2O$ in EtOH at ambient temperature and under argon. Ethanol was chosen in order to avoid deleterious transesterification reactions that could occur with a different alcohol. The resulting blue solution containing *ca.* 11% EtOH became problematic with a moiré-effect under stirring. Evaporation of the two solvents to dryness afforded a blue solid that was taken in CH_2Cl_2, giving an insoluble material. After trituration, filtration, and rinsing, this insoluble material afforded the complex **3** with a yield of 82%.

In parallel, the reference 6′6′-dimethyl-2,2′-bipyridyl)$Co(Cl)_2$ complex **4** (dmbp$CoCl_2$) was prepared as a deep-blue green microcrystalline solid by reaction of 1 equivalent of $CoCl_2{\cdot}6H_2O$ in MeOH with 6,6′-dimethyl-2,2′-bipyridine in $CHCl_3$.[36]

The ligand **2** was fully characterized by UV-vis and infrared spectroscopy, ^1H and ^{13}C-NMR spectroscopy, electrospray mass spectrometry, and combustion analysis. The results obtained were fully consistent with the proposed formula. The tetra cobalt(II) complex **3** was analyzed by UV-visible (titration and final characterization) and infrared spectroscopy. The combustion analysis was consistent with the proposed formula involving the presence of 3 complementary molecules of H_2O. Results from the positive mode ESI mass spectrometry were consistent with the mono-, di- and tri-charged species incorporating ligand **2** and cobalt, but without expression of the molecular peak.

As previously explored,[27] 1D (^1H-, ^{13}C-) and 2D (COSY, HSQC) NMR spectroscopies were employed to analyze the paramagnetic complex.

UV-Visible titration

The blue color of complex **3** indicates that cobalt(II) is in a tetrahedral environment, favored by the steric hindrance generated by the bipyridyl 6-methyl and 6′-methylene groups and the two coordinating chlorides. The complexation of the ligand **2** by cobalt(II) was followed by UV-visible-near infrared titration between 250 and 1000 nm, of 3 mL of a 1.006×10^{-5} M CH_2Cl_2 solution of **2**, with *ca.* 50 μL of a 2.412×10^{-3} M ethanolic solution of $CoCl_2{\cdot}6H_2O$.

The results given in Fig. 1 show that the complexation is finalized at the 10th aliquot (50 μL) of $CoCl_2$ solution, *i.e.*, 4 equivalents, which is consistent with the expected M_4L stoichiometry. Three main domains of transitions are visible.

The first one, in the UV-visible region of 250–450 nm (Fig. 2), is representative of effects of cobalt complexation on the bipyridyl chelating moieties. Notably, disappearance of the π–π* transition of the ligand centered at 292 nm (Abs = 0.686, $\varepsilon = 68\,224$ mol^{-1} L cm^{-1}) to the benefit of a bathochromically shifted envelope including a new band at 317 nm (Abs = 0.446, $\varepsilon = 44\,356$ mol^{-1} L cm^{-1}) and a shoulder at *ca.* 343 nm (Abs = 0.214, $\varepsilon = 21\,312$ mol^{-1} L cm^{-1}) confirms the successful coordination.

Two isosbestic points are observed at 308 nm (0 to 25 μL–0 to 2 equivalents of metal ion) and 301 nm (30 to 50 μL–2.4 to 4 equivalents of metal ion) (Fig. 3). Despite the poor resolution, the isosbestic points suggest the formation of the LM and LM_2 species at 308 nm and LM_3 and LM_4 at 301 nm.

The second domain, between 500 and 750 nm, is presented in Fig. 4. As in previous reports,[27,29,36] it shows two weak transitions

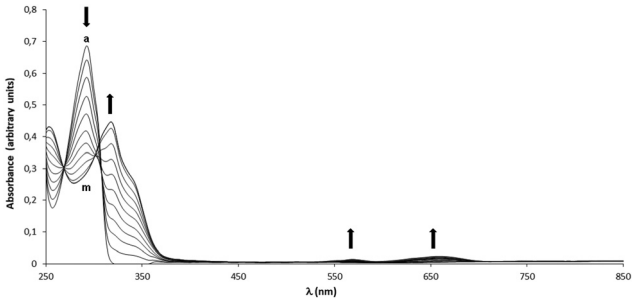

Fig. 1 UV-vis titration of ligand **2** (3 mL at 1.006×10^{-5} M in CH_2Cl_2) by a solution of $CoCl_2{\cdot}6H_2O$, 2.412×10^{-3} M in EtOH. Wavelength window: 250–850 nm. (a) Pure ligand **2**, (b)–(k): pure **2** plus 5 μL aliquots of $CoCl_2$ solution up to 50 μL; (l) and (m) 55 and 60 μL. Equivalence was achieved at 50 μL of Co(II) solution.

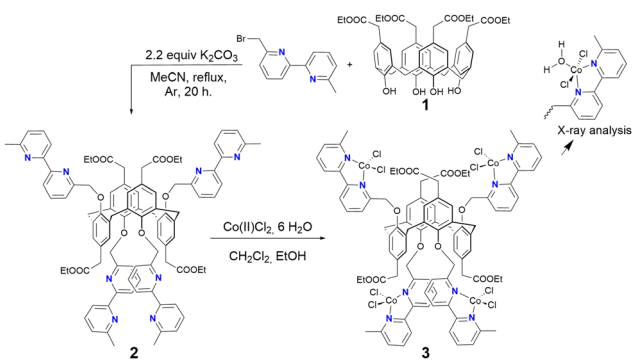

Scheme 1 Synthetic pathway to complex **3**.

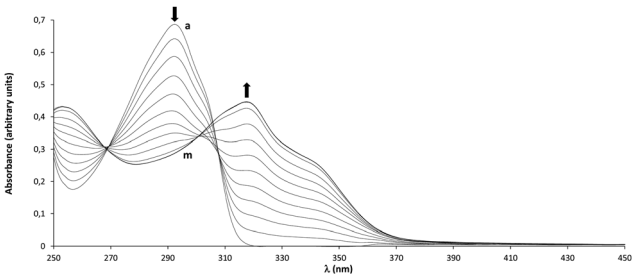

Fig. 2 UV-Vis titration of ligand **2** (3 mL at 1.006×10^{-5} M in CH_2Cl_2) by a solution of $CoCl_2{\cdot}6H_2O$, 2.412×10^{-3} M in EtOH. Wavelength window: 250–450 nm. (a) Pure ligand **2**, (b)–(k) pure **2** plus 5 μL aliquots of $CoCl_2$ solution up to 50 μL; (l) and (m) 55 and 60 μL. Equivalence was achieved at 50 μL of Co(II) solution.

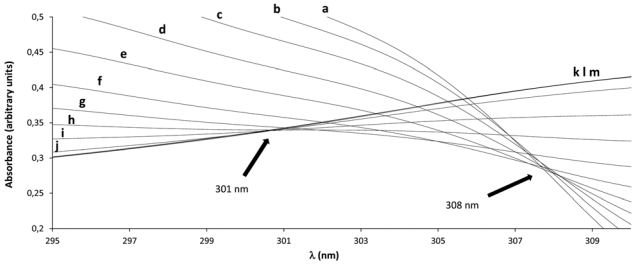

Fig. 3 UV-Vis titration of ligand **2** (3 mL at 1.006×10^{-5} M in CH_2Cl_2) by a solution of $CoCl_2{\cdot}6H_2O$, 2.412×10^{-3} M in EtOH. Isosbestic points wavelength window: 295–310 nm. (a) Pure ligand **2**, (b)–(m) pure **2** plus 5 μL aliquots of $CoCl_2$ solution.

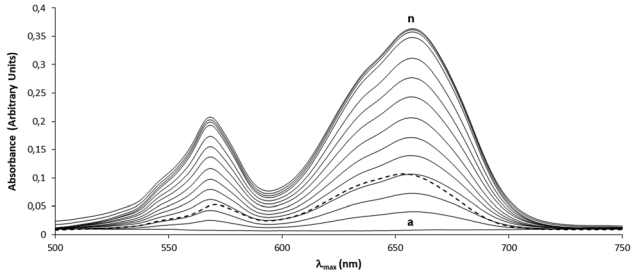

Fig. 4 UV-Vis titration of ligand **2** (3 mL at 2.011×10^{-4} M in CH_2Cl_2) by a 4.825×10^{-2} M solution of $CoCl_2{\cdot}6H_2O$ in EtOH. Wavelength window: 500–750 nm. (a) Pure ligand **2**, (b)–(k) pure **2** plus 5 μL aliquots of $CoCl_2$ solution up to 50 μL; (l)–(n) 55, 60 and 65 μL. Equivalence was achieved at 50 μL of Co(II) solution (here between 50 and 55 μL). Black dashed line: UV-visible spectrum of Co(dmbpy)$(Cl)_2$ complex **4** in CH_2Cl_2 at 2.011×10^{-4} M.

with maxima at 569 nm (Abs = 0.198, ε = 985 mol^{-1} L cm^{-1}) and 658 nm (Abs = 0.357, ε = 1775 mol^{-1} L cm^{-1}), which are attributed to metal-to-ligand-charge-transfer (MLCT) and d–d metal-centered-transitions (MCT), respectively. The low absorptivity of those transitions required titration with a solution that was 20 times more concentrated (2.011×10^{-4} M for **2** and 4.825×10^{-2} M for the cobalt salt solution).

Finally, a transition of very low intensity is present in the near infrared region at 966 nm (not shown on figures). This transition increased regularly with the addition of cobalt solution, and was characterized by a molar extinction coefficient of 160 mol^{-1} L cm^{-1}, *i.e.*, 40 by final Co/bipyridyl subunit.

The bold dashed line present in Fig. 4 corresponds to the (6,6′-dimethyl-2,2′-bipyridyl)Co$(Cl)_2$ complex **4** (dmbp($CoCl_2$) in the visible region. It reveals the existence of similar transitions, located at λ_{max} 571 nm (Abs = 0.053, ε = 262 mol^{-1} L cm^{-1}) and λ_{max} 654 nm (Abs = 0.106, ε = 530 mol^{-1} L cm^{-1}), corresponding to transitions centered on a tetrahedral cobalt ion complexed by the 6,6′-dimethyl-2,2′-bipyridine moiety and two chlorine anions. Its similarity with curve d (third line over a) is in accordance with the first global equivalence during the formation of complex **3** (1.2 equivalents of $CoCl_2$).

These observations point toward a CoA2B2 symmetry tetrahedral geometry around the cobalt ion, according to Banci *et al.*[41] Of note, the same authors assume that a pentacoordination around Co(II) high spin generates transitions in the same range as our results with a characteristic transition at 625 nm within the envelope of the visible spectrum of **3**, and also of **4** between 600 and 700 nm. Thus, it is possible that a part of Co/bipyridyl subunits in **3** is pentacoordinated in solution. This will be demonstrated by X-ray diffraction study in the solid state. On the basis of empirical approaches from spectroscopic and structural concordance studies, Bertini[42] and Sartorius *et al.*[43] assumed that transitions in the 500–700 nm region with an ε value inferior to 50 mol^{-1} L cm^{-1} correspond to a pseudooctahedral hexacoordination around high-spin Co(II). Meanwhile, ε values between 50 and 200 mol^{-1} L cm^{-1} would rather indicate a pentacoordination with variable geometry. Finally, ε values greater than 300 mol^{-1} L cm^{-1} corresponded to a pseudotetrahedral tetracoordination. Between these domains, or at the borderlines, two geometries can be proposed.

Following these rules, we suggest herein that complex **4** adopts a tetrahedral geometry due to its transition at ε_{654} = 530 mol^{-1} L cm^{-1}, as with complex **3**, for which the value of ε_{658} = 443 mol^{-1} L cm^{-1} by the bpy$CoCl_2$ unit is observed.

Infrared spectroscopy

Infrared spectroscopy was performed in ATR mode (diamond) between 4000 and 400 cm^{-1} (2500, 25 000 nm) (Fig. S1, ESI†) on the reference ligand 6,6′-dimethyl-2,2′-bipyridine (dmbp), the reference cobalt complex 6,6′-dimethyl-2,2′-bipyridyl(Co$(Cl)_2$) **4** (dmbp($CoCl_2$)), on crystals of complex **3** and on the free ligand **2**. No relevant bands were observed in the region 4000–2000 cm^{-1}. Thus, only the spectra in the 2000–400 cm^{-1} region are given in Fig. 5.

Comparison of the free ligand **2** (spectrum a) and free dimethylbipyridine (spectrum d) shows good homology around 780 cm^{-1} (C═C–H with two C–H neighbors), 1438 cm^{-1} (C═C–H deformations, CH_3 elongations) and 1572 cm^{-1} (pyridyl C═N, C═C valence vibrations). In addition, ligand **2** displays two other major bands at around 1148 cm^{-1} (calixarenic C–O ester and ether) and 1730 cm^{-1} (C(O)OEt functions).

For the bipyridyl complex **4** (spectrum c), we notably observe the splitting of the bipyridyl band at 1571.98 cm^{-1} into a sharp band at *ca.* 1599 cm^{-1}. This is attributed to the pyridyl C═N being directly impacted by the complexation to cobalt ion. The two remaining ones at around 1560 and 1566 cm^{-1} are attributed to calixarene C═C valence vibrations. Similar transformations are observed for complex **3** (spectrum b), for which we also observe an impact of cobalt complexation on the sharp and intense ester band at 1730 cm^{-1} in ligand **2**. This evolves towards a more complex structure, suggesting a possible interaction between the cobalt/bipyridyl subunits and carboxylates due to their proximity caused by the 1,3-alternate conformation.

NMR spectroscopy

As previously shown with some parent paramagnetic cobalt(II) complexes of bipyridyl calixarenes,[27,29] NMR spectroscopy was useful to attempt elucidation of the structure of complex **3**. The (6,6′-dimethyl-2,2′-bipyridyl)Co$(Cl)_2$ complex **4** served as reference for the chemical shifts of the bipyridine units.

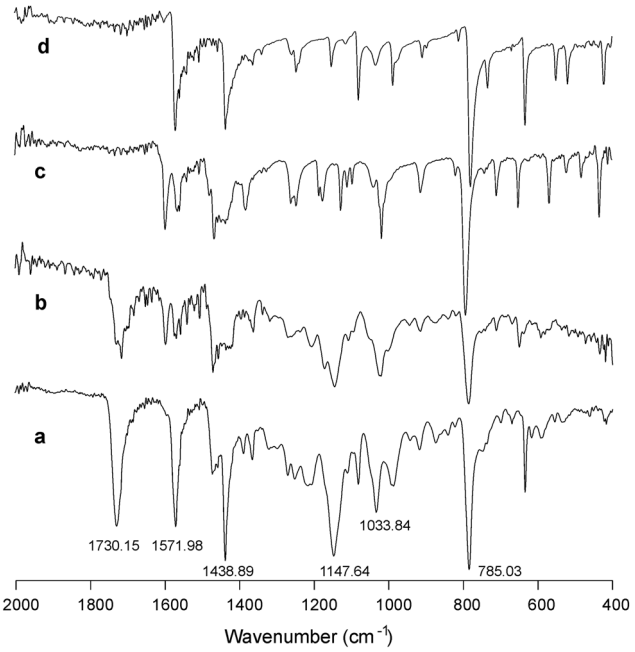

Fig. 5 2000–400 cm^{-1} FTIR (ATR mode) spectra of (a) ligand **2**, (b) crystals of tetranuclear complex **3**, (c) microcrystalline dmbp($CoCl_2$) complex **4**, and (d) 6,6′-dimethyl-2,2′-bipyridine (dmbp).

Thus, in $CDCl_3$ (Fig. S2c, ESI†), the symmetric complex **4** displays 4 resonance signals spread between 80 and −40 ppm. These features are characteristic of the paramagnetic influence of Co(II): three singlets at 69.75, 47.23 and −15.03 ppm integrating to 2 H each and with half-value widths of *ca.* 19 Hz, which were attributed to the six bipyridyl aromatic protons, and one broad singlet strongly upfield shifted at *ca.* −21 ppm, integrating to 6 H with an important half-value width of 145 Hz, attributed to the methyl groups.

For the tetranuclear complex **3**, 1D (^{1}H-; ^{13}C-) and 2D (COSY, HSQC) experiments were employed. 1D ^{1}H-NMR was realized with a solution of **3** in a mixture of CD_3CN and CD_2Cl_2 at RT between 80 and −50 ppm. The 1D spectrum reveals the high symmetry of **3** in solution (Fig. 6), exhibiting 13 relevant signals. Four signals occur in the very low fields at *ca.* 74.1, 67.2, 53.8 and 32.0 ppm, with half-value widths between 35 and 25 Hz and integration of 4 H each. In addition to the solvent resonance signals at 5.42 and 1.96 ppm in the normal fields, two resonance signals appear at *ca.* 7.4 and 4.3 ppm, with half-value widths of close to 20 Hz and integrations of 8 and 12 H, respectively. In the high to very high fields, seven resonance signals appear at *ca.* −1.3, −3.7, −8.4, −15.0, and −19.2 ppm, with half-value widths comprising between 14 and 50 Hz, integrating for 8, 8, 8, 4 and 4 H, respectively, and at *ca.* −22.9 and −44.9 ppm with larger half-value widths of *ca.* 250

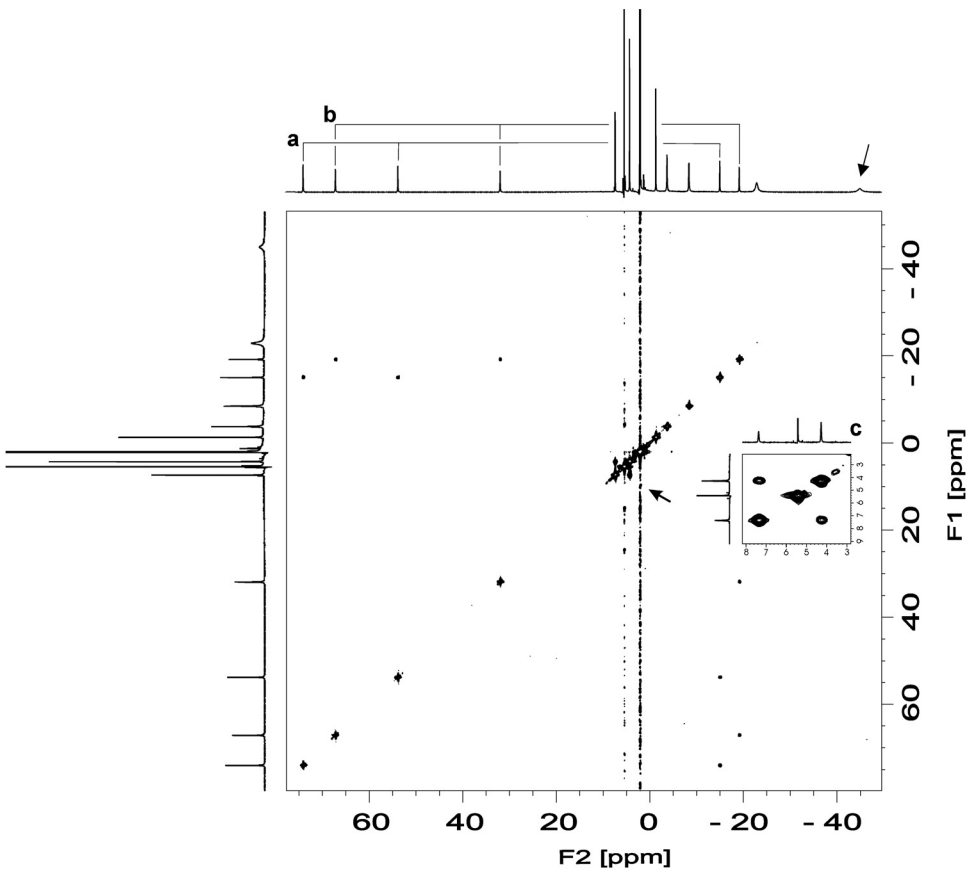

Fig. 6 COSY NMR experiment on complex **3** in CD_3CN + CD_2Cl_2 (**a** and **b** refer to pyridyl subunits description).

and 400 Hz, integrated to 12 and 8 H, respectively. The COSY experiment (Fig. 6) exhibits two triads at 74.07, 53.81, −15.00 and 67.16, 31.95, −19.18 ppm that were attributed to pyridyl aromatic protons,[29] although their exact distribution within the biheterocycle was unclear.

According to the upfield shifting effect of the paramagnetic cobalt(II) on the CH_3 groups of complex **4**, and on the basis of the integration values, the two large resonance signals at *ca.* −22.9 and −44.9 ppm correspond to the bipyridyl CH_3- and CH_2O-groups, respectively. Unfortunately, no long range COSY correlation with their close aromatic protons were found.

With respect to their integrations, a correlation between the two abovementioned signals at *ca.* 7.4 and 4.3 ppm confirmed their attribution to the ethyl ester groups. Of note, their unusual chemical shifts suggest they are under the paramagnetic influence of cobalt(II) (Fig. 6, inset).

With the help of the ^1H,^{13}C-HSQC experiment (Fig. S3, ESI†), the three residual resonance signals integrated to 8 H each at −8.43, −3.73 and −1.33 ppm were attributed to the bridging methylene groups (ArCH_2Ar), the calixarenic aromatic protons (Ar*H*) and the acetyl methylenes (OCH_2C(O)OR), respectively.

Because of the lack of solubility of **3** and **4** in pure or mixed $CDCl_3$, CD_2Cl_2, CD_3OD or CD_3CN, the ^{13}C-NMR analysis carried out between −40 and 800 ppm[44] showed a low signal-to-noise ratio, making it difficult to interpret.

The d_6-DMSO was found to decomplex cobalt from bipyridine (loss of the characteristic blue colour and release of free bipyridine in solution). However, (*H*)DMF apparently did not, and afforded (as with pure $CoCl_2{\cdot}6H_2O$) deep blue solutions of **3** and **4** with higher concentrations. The proton-coupled ^{13}C-NMR analysis of **4** (Fig. S4, ESI†) exhibited 6 resonance signals of equal integrations, comprising 3 doublets at 295.13, 313.24 and 475.2 ppm, with J_{H-C} values of 170 Hz, corresponding to pyridyl *C*H, and two broad signals at 348.00 and 362.00 ppm which were attributed to the four quaternary carbons. The absence of quartet multiplicity for the CH_3 signal at 138.79 ppm may be due to the half-value width (145 Hz) of its ^1H-resonance signal.

Unfortunately, no data related to a paramagnetic cobalt complex were obtained with complex **3**, with weak and badly resolved resonance signals located between 0 and 180 ppm that may correspond to the released ligand.

To overcome the solubility and concentration constraints, we attempted a ^1H,^{13}C-HSQC experiment in a mixture of CD_3CN and CD_2Cl_2 between −100/+300 ppm and −30/+80 ppm for the carbon and proton dimensions, respectively. The 2D spectrum thus obtained (Fig. S3, ESI†) exhibited well-defined correlations for the solvent and for some calixarene fragments in the 0 to 130 ppm ^{13}C- and −5 to +10 ppm ^1H-region. No other correlations, notably for the ^1H resonance signals of bipyridines, were found.

The ^{13}C-characterization of complex **3** was finally obtained in a CD_3CN + $CDCl_3$ mixture, with an accumulation period of 72 h,

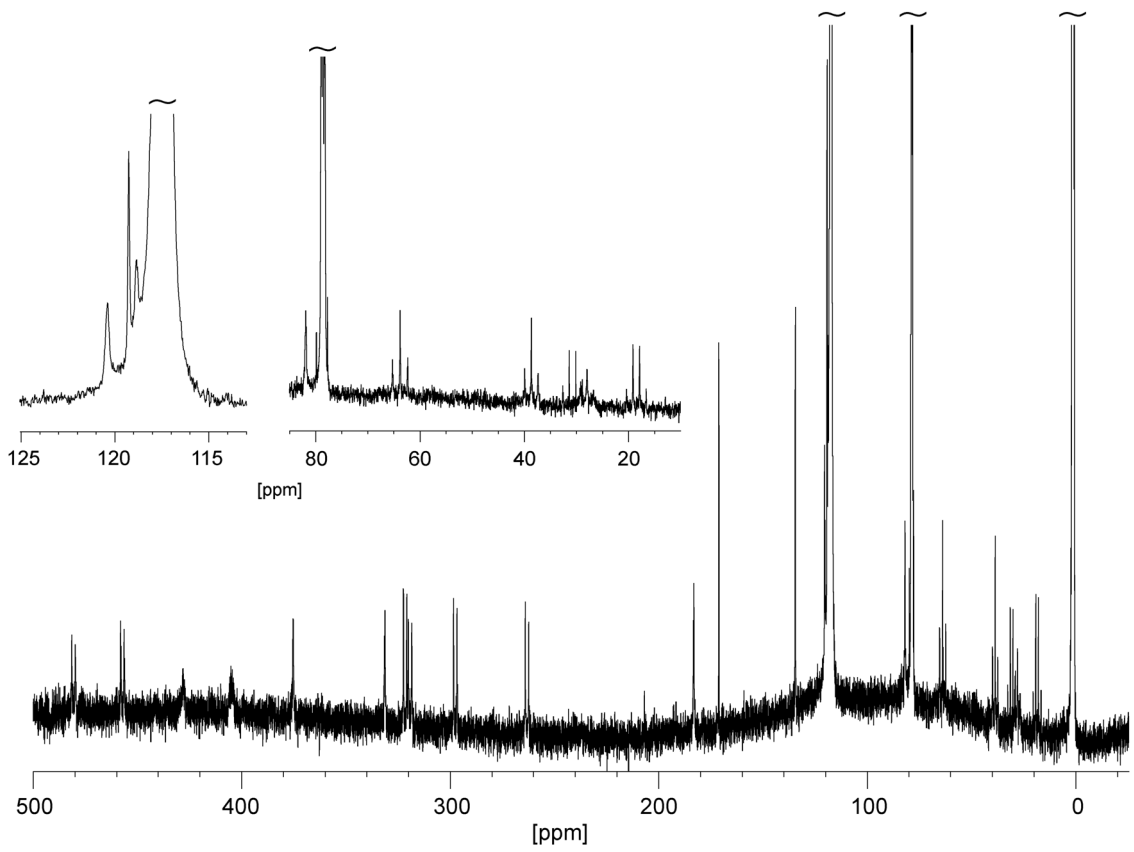

Fig. 7 ^{13}C-NMR spectrum of complex **3** (RT, CD_3CN, $CDCl_3$, 72 h; selected window: 500 to −25 ppm).

between 700 and −100 ppm. Resonance peaks were found in the window of 500 to −25 ppm, as represented in Fig. 7 and described in the Experimental section.

X-Ray diffraction analysis

Complex **3** crystallizes as blue parallelepipedic single crystals by slow evaporation of an acetonitrile/CH_2Cl_2 solution.

The structure was solved at 90 K, and Table 1 summarizes the relevant information on the data collection and structure refinements.

The last refinements give rise to the formula $C_{92}H_{88}Cl_8Co_4N_8O_{13}$ with $Z = 2$.

The odd number of oxygen atoms, *i.e.*, 13, is due to the presence of one supposed molecule of water attached to one of the four cobalt centers. As no hydrogen atom can be positioned with certainty, the choice between the neutral water molecule or the anionic hydroxyl group as the ligand must take into account the presence of a cobalt(II) or a cobalt(III) species, respectively, which will be discussed.

This analysis also confirms the coordination sphere of the three complex subunits, named **Co1bpyCl$_2$**, **Co2bpyCl$_2$**, and **Co3bpyCl$_2$**, which adopt a pseudo-tetrahedral geometry. Remarkably, the fourth unit **Co4bpyCl$_2$(O)** is a trigonal bipyramidal penta-coordinated species involving an oxygen ligand (O41), in addition to the two bipyridyl nitrogen atoms and the two chlorine anions.

Table 1 Summary of single-crystal data collection and structure refinement conditions of complex **3**

Structural formula	$C_{92}H_{88}Cl_8Co_4N_8O_{13}$
Space group	$P\bar{1}$
Temperature [K]	90(2)
Formula weight	2033.1
Wavelength (Å)	0.71073
Crystal system	Triclinic
Crystal colour	Blue
Unit cell dimensions	
a [Å]	13.1367(19)
b [Å]	16.011(2)
c [Å]	23.770(4)
α [°]	75.598(4)
β [°]	83.619(5)
γ [°]	71.724(4)
V [Å^3]	4595.2(12)
Z	2
Crystal description	Parallelepiped
Calculated density (g cm^{-3})	1.469
Absorption coefficient [mm^{-1}]	1.008
F(000)	2088
Crystal dim [mm]	0.2 × 0.2 × 0.4
Theta range [°]	3–24
h_min, h_max	−12, 12
k_min, k_max	−14, 14
l_min, l_max	−21, 21
R(int)	0.085
Reflections collected	76 342
Reflections unique	7572
Data/restraints/parameters	7572/0/1109
Goodness-of-fit	1.07
Final R value	0.062 for 7572 data
Final R_1 [$I > 4\sigma$]	0.041 for 5930 data
Final wR_2 [$I > 4\sigma$]	0.0904
Largest difference [e Å^{-3}]	0.41 and −0.30

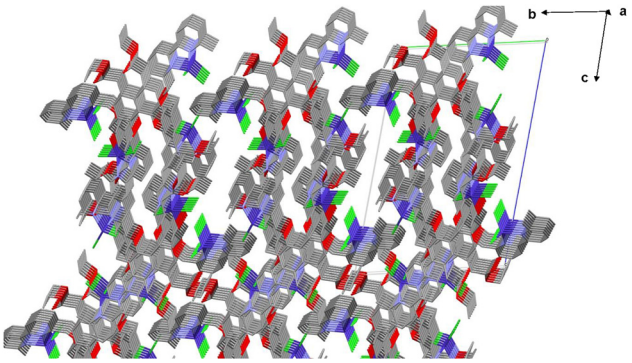

Fig. 8 Crystal packing at 90 K of complex **3** (capped sticks, no hydrogens) along the *a*-axis (6.5 layers), *b*-axis (3 layers) at the left, and *c*-axis (2 layers) down.

Fig. 8 shows the crystal packing of complex **3** at 90 K and the voluminous solvent-accessible (but empty) void volume estimated to be 86 Å^3 by the unit cell (*ca.* 2% of the cell volume).

Fig. 9 presents the two molecules of complex **3** within one unit cell, and confirms the 1,3-alternate conformation of the calix[4]arene platform foreseen from ^{1}H- and ^{13}C-NMR analyses of the ligand **2**, with ArCH$_2$Ar singlet resonance signals at 3.75 and 37.45 ppm, respectively. As expected, the calixarene platform bears four dimethylbpy($CoCl_2$) subunits, each attached to the platform *via* an oxa-methylene arm.

Fig. 10 and Table S1 (ESI†) show the quasi-perfectly square-tubular structure of the calixarene platform, with the four phenyl rings found parallel to their alternate parent, and in the prolongation along the C2 axis, orthogonal to their spanning ones. The pairs **Co1bpyCl$_2$**/**Co3bpyCl$_2$** and **Co2bpyCl$_2$**/**Co4bpyCl$_2$(O)** are found in alternate position on opposite sides of the calixarene core.

From Fig. 10 and 11, it can be seen that the **Co1bpyCl$_2$** unit is aligned perpendicular to its tethered phenolic unit, with $CoCl_2$ oriented to the phenyl side. **Co2bpyCl$_2$** and **Co4bpyCl$_2$(O)** are aligned almost perpendicular to their tethered phenolic units, with their $CoCl_2$ oriented also on the phenyl side. However, **Co2bpyCl$_2$** leans 15 degrees to the plane of its phenyl group, and is oriented towards the face of **Co1bpyCl$_2$**. Meanwhile, **Co4bpyCl$_2$(O)** leans 12 degrees to the plane of its phenyl group, and is oriented towards the face of **Co3bpyCl$_2$**. Finally, the latter is oriented with an angle of *ca.* 124° with respect to its tethered phenyl ring.

Geometries around cobalt ions. Geometric parameters related to these subunits are described in Tables 2–4 and Table S2 (ESI†).

The tetrahedral geometry of **Co1**, **Co2** and **Co3** is comparable with the crystallographic data available for the free (6,6′-dimethyl-2,2′-bipyridyl)Co(Cl)$_2$ complex **4**,[45,46] and with the parent complexes previously published by our group.[27,29] The three bipyridine units are slightly distorted in terms of planarity, with the N–C–C–N dihedral angles comprising between 4 and 7 degrees, showing the adaptation of the biheterocycles to the strained tetrahedral geometry.

Co4 adopts a trigonal bipyramid geometry, likely preferred due to the coordination of a fifth, oxygen-based, ligand.

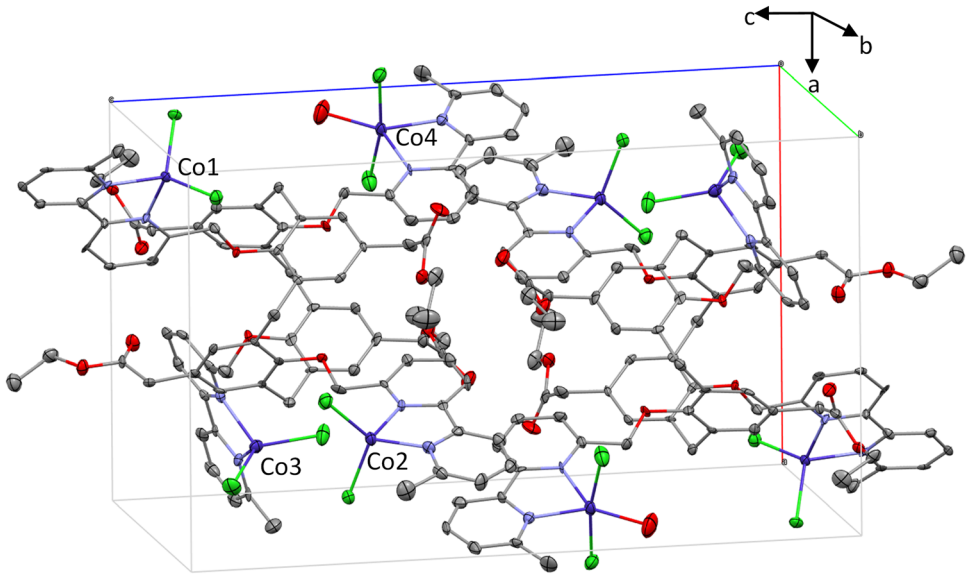

Fig. 9 The two molecules of the complex **3** in the unit cell at 90 K. ADPs ellipsoids at 50% probability level.

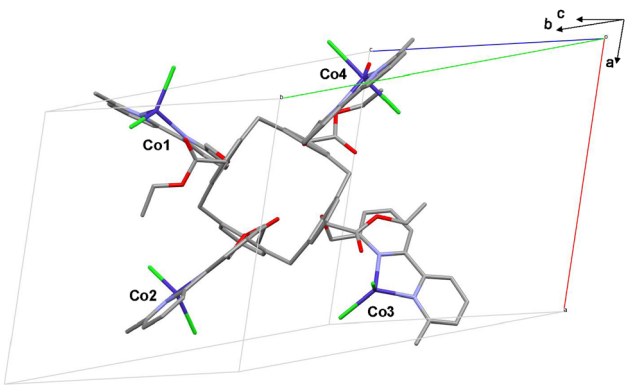

Fig. 10 Focusing on the square-tubular section structure of the calixarene at 90 K.

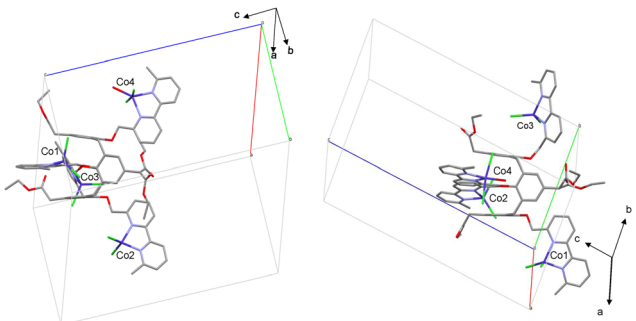

Fig. 11 C2 axis oriented lateral views of: (left) Molecule 1 and (right) molecule 2 of complex **3** in the unit cell at 90 K.

This ligand completes the coordination sphere along with the two bipyridyl nitrogens (N41 and N42) and its oxygen atom (O41) found in a N41,N42-pinched triangular base, and the two chloride anions (Cl41 and Cl42) opposed at the apexes of each pyramid.

Thus, angles measured around **Co4** in the triangular base are 78.5° for N41–Co4–N42, and 136.6° and 145.0° for O41–Co4–N41 and O41–Co4–N42, respectively. The chlorine atoms slightly lean towards the calixarene platform, with angles of *ca.* 85° with respect to O41, and form an angle of only 169.50°, which is far from the expected 180°.

Surprisingly, no similar geometry with bipyridine-based cobalt(II) complexes was found in the literature. The closest structure, proposed by Tran and Marsura,[47] involves the 6-methyl-6′-[2-oxa-propylbipyrazinyl]-2,2′-bipyridine ligand. The complexation of cobalt(II) is achieved by the two bipyridyl nitrogen atoms, two chlorine anions and the oxygen of the oxapropyl arm, in a penta-coordinated mode, with adoption of a distorted tetrahedral geometry capped by the ether oxygen at *ca.* 2.4 Å from cobalt. In this case, the degrees of freedom along the sigma bonds allows the positioning of this ether oxygen near the cobalt center. In our case, the steric hindrance of the calixarene moiety prevents such an orientation of the corresponding analogous phenoxy oxygen in complex **3**.

Sykes *et al.*[48] described another example involving the rigid phenanthroline ligand. This mono-phenanthrolyl, dichloro, mono DMSO cobalt(II) complex displays a penta-coordinate structure intermediate between the trigonal bipyramidal and square pyramidal geometries, where the two N_{phen} atoms are adjacent, the two chlorines are perpendicular from each other, and the DMSO ligand occupies the fifth position *via* one of its oxygens. Gennari and Duboc described a bipyridine functionalized by two thiol arms, and its Co(II) (dimeric: 2 N_{bpy} plus 2 bridging S and 1 bridging S–S by Co) or Co(III) (monomeric, 2 N_{bpy} plus 2 bridging S, 1 Cl) centers, each penta-coordinated with a distorted square pyramidal geometry.[49,50]

Other pentacoordinations of cobalt(II) have been also described with terpyridine and analogous ligands, which we nevertheless considered too far from bipyridine.[51–53]

Table 2 Selected geometric parameters in [bipyridine($CoCl_2$)] subunits

Bond lengths around cobalt(II) centres [Å]			
Co1 Unit		Co2 Unit	
N11–Co1	2.034(4)	N21–Co2	2.050(5)
N12–Co1	2.049(5)	N22–Co2	2.018(5)
Cl11–Co1	2.211(2)	Cl21–Co2	2.211(2)
Cl12–Co1	2.202(2)	Cl22–Co2	2.219(2)
Co3 Unit		Co4 Unit	
N31–Co3	2.031(5)	N41–Co4	2.066(5)
N32–Co3	2.006(5)	N42–Co4	2.079(5)
Cl31–Co3	2.217(2)	Cl41–Co4	2.366(2)
Cl32–Co3	2.220(2)	Cl42–Co4	2.362(2)
		O41–Co4	2.057(4)
Bond angles around cobalt(II) centres [°]			
Co1 Unit		Co2 Unit	
N11–Co1–N12	79.7(2)	N21–Co2–N22	81.0(2)
N11–Co1–Cl11	111.40(13)	N21–Co2–Cl21	109.66(14)
N11–Co1–Cl12	119.01(14)	N21–Co2–Cl22	112.74(14)
N12–Co1–Cl11	111.08(13)	N22–Co2–Cl21	109.66(14)
N12–Co1–Cl12	116.53(13)	N22–Co2–Cl22	122.22(15)
Cl11–Co1–Cl12	114.43(7)	Cl21–Co1–Cl22	116.96(07)
Co3 Unit		Co4 Unit	
N31–Co3–N32	81.3(2)	N41–Co4–N42	78.5(2)
N31–Co3–Cl31	116.21(14)	N41–Co4–Cl41	93.14(13)
N31–Co3–Cl32	113.10(14)	N41–Co4–Cl42	96.40(14)
N32–Co3–Cl31	115.10(14)	N42–Co4–Cl41	92.94(13)
N32–Co3–Cl32	116.48(14)	N42–Co4–Cl42	93.28(13)
Cl31–Co3–Cl32	111.63(7)	Cl41–Co4–Cl42	169.49(7)
		O41–Co4–Cl41	85.42(14)
		O41–Co4–Cl42	84.23(14)
		O41–Co4–N41	145.0(2)
		O41–Co4–N42	136.6(2)

Table 3 Distortion of bipyridine subunits [°]

Co1 Unit		Co2 Unit	
C15–C16–C17–C18	−6.0(1)	C25–C26–C27–C28	−9.0(1)
N11–C16–C17–N12	−4.0(8)	N21–C26–C27–N22	−8.4(8)
Co3 Unit		Co4 Unit	
C35–C36–C37–C38	4.0(1)	C45–C46–C47–C48	1.0(1)
N31–C36–C37–N32	2.2(8)	N41–C46–C47–N42	1.0(8)

Status of the O41 atom. The presence of the fifth oxygen ligands on the **Co4** entity in complex **3** can be associated with either a hydration process conserving the Co(II) status, or a hydroxylation reaction, passing thus from Co(II) to Co(III).

The crystallization is realized by slow evaporation of the solvent, without specific protection from air, *i.e.*, oxygen and water. However, the presence of water molecules inherent to the hexa aquo cobalt(II) salt used for complexation led us to the conclusion that this fifth ligand is H_2O.

Due to the oxygen orientation, at least one of its hydrogen atoms could be involved in hydrogen bonds with the chlorine atoms of the **Co3bpyCl$_2$** subunit located in the neighbor cell (see Fig. 13), thus participating in the crystal cohesion/edification.

Of note, the divalent or trivalent status of **Co4** could be linked to the fact that Co(II) should generate longer bonds with coordinating atoms than Co(III), due to their ionic radii.[54]

Surprisingly, to the best of our knowledge, no data related to Co(II) complexes involving H_2O as the ligand were found. Meanwhile, one structure involving the monodentate –OH group attached to an octahedral Co(III) complexed by a bispidine has been described by Comba *et al.*,[55] with the Co(III)–OH distance measured at 1.958 Å, 2.3% smaller than that of **Co4**–O.

A focus on bipyridine ligands and on their cobalt complexes gave interesting results on nitrogen–cobalt distances.

For example, the two bisthiolato-bipyridyl pentacoordinated Co(II) or Co(III) complexes reported by Gennari and Duboc show two *d*Co(III)–N_{bpy} value of 1.9915 and 2.0267 Å for the Co(III) species. Meanwhile, the distances in its reduced form increase to *d*(Co(II)–N_{bpy}) of 2.072 and 2.11 Å, respectively.[49,50] Reimann *et al.* gave two *d*Co(III)–N_{bpy} values of 1.922 and 1.936 Å for a bis-bipyridyl, nitrato Co(III) octahedral complex, close to those of Gennari's species.[56] Sengottuvelan *et al.* showed *d*Co(III)–N_{bpy} values of 1.9294(15) and 1.9186(18) Å for the octahedral hexacoordinated [Co(acac)(bpy)$(N_3)_2\cdot H_2O$] complex.[57] Similar N_{bpy}–Co(III) distances comprising between 1.920 and 1.940 Å were described by Talwar *et al.* for the distorted octahedral hexacoordinated $[Co(bpy)_2CO_3]\cdot IO_4$ complex.[58]

More interesting for our purpose, Toyama *et al.* described N_{bpy}–Co(III) distances of 1.929(2) and 1.919(2) Å for the octahedral hexacoordinated *cis*-$[Co(bpy)_2(OH_2)_2][OTf]_3\cdot H_2O$ complex species involving two 2,2′-bipyridines in the *cis*-position, and two coordinating H_2O molecules. The distances between the oxygen atoms of these water molecules and the Co(III) center are not discussed, but examination of the cif file shows that they measure at 1.913(14) Å each, 7.5% shorter than O41–**Co4** (2.057(4) Å).[59]

Table 4 Particular geometric parameters in subunit Co4 of complex **3**

Distances around **Co4** at the unit cell interface (along the *c* axis) [Å]					
Co4–(Co3)′	5.700(1)	Cl41–(Cl31)′	4.801(3)	O41–(Cl31)′	3.302(6)
Cl41–(Co3)′	6.124(2)	Cl41–(Cl32)′	5.680(2)	O41–(Cl32)′	3.223(4)
Cl42–(Co3)′	5.879(2)	Cl42–(Cl31)′	5.075(3)	Co4–(Cl31)′	4.467(2)
O41–(Co3)′	3.906(5)	Cl42–(Cl32)′	5.491(2)	Co4–(Cl32)′	5.278(2)
Angles around **Co4** at the unit cell interface (along the *c* axis) [°]					
(Cl31)′–Co4–(Cl32)′	43.27(3)	(Co3)′–(Cl31)′–O41	87.8(1)		
(Cl31)′–Co4–(Co3)′	21.05(2)	(Co3)′–(Cl32)′–O41	89.7(1)		
(Cl32)′–Co4–(Co3)′	22.92(2)	(Cl31)′–O41–(Cl32)′	68.5(1)		

Through these results, we see that the average distance between cobalt(III) and bipyridyl N chelating atoms is about 1.94 Å, compared to the cobalt(II) species of Gennari at 2.07 Å, which is close to the distance dCo4–N_{bpy} values measured at 2.066 and 2.075 Å in complex **3**. This allows us to describe **Co4** as a pentacoordinated Co(II) species, indicating that the oxygen-containing fifth ligand must be neutral, *i.e.*, a coordinating molecule of H_2O.

Presence of hydrogen bonds around Co4. Fig. 12 presents two molecules of complex **3** arranged in two adjacent cells along the *a*-axis. It shows that the **Co4 bpyCl$_2$(O)** subunit of the main unit cell looks towards the **(Co3bpyCl$_2$)′** subunit of the adjacent cell, of which cobalt is represented as **(Co3)′**.

Assuming the aqueous nature of O41, this part of the crystal is possibly the place of crystal stabilizing interactions; for example, *via* hydrogen bonding between hydrogen(s) attached to O41 and neighbor chlorine ions. This hypothesis is consistent with the work of Steiner.[60] With help of the CSD database and considering the O–H bond length at 0.983 Å, Steiner related that, for H_2O bonded to a transition metal atom, the H-bond with the Cl anion has a mean length of 2.182(8) Å and the mean O···Cl anion distance is 3.190 Å, if the angle at H is $>140^\circ$ and the directionality O–H–Cl is in the range of over 140° to 180°.

More recently, Pethes *et al.* showed that a H-bond between H_2O and the Cl anion is acceptable if the H···Cl anion is less than 2.8 Å, and the angle Cl–O–H is smaller than 30 degrees.[61]

According to Fig. 13 and Table 5, a model drawing was prepared (Fig. 14) in which two hydrogen atoms are added to O41, respecting the distances H···O of 0.983 Å and the H–O–H angle of 104.5°. This modelling approach, even if poor scientifically, allows the building of a precession cone around O41 at the summit and with the two H (Ha and Hb) on the large rim. Their positioning is arbitrarily symmetrical with regards to the O41–Co3′ axis, and within the Cl32′–O41–Cl31′ plane. This give the Ha···Cl32′ and Hb···Cl31′ distances of 2.30 Å and 2.36 Å, respectively, which are inferior to the maximum limit of 2.80 Å described by Pethes, but slightly greater than the 2.182 Å given by Steiner.

The Cl32′–O41–Ha and Cl31′–O41–Hb angles of 17° and 18°, respectively, are inferior to the maximum limit of 30° given by Pethes. Meanwhile, the O41–Ha–Cl32′ and O41–Hb–Cl31′ angles of 157 and 155°, respectively, are within the 140° and 180° limits given by Steiner. The O41···Cl32′ and O41···Cl31′ distances of 3.223 Å and 3.302 Å, respectively, are slightly greater than the mean distance value of 3.190 Å given by Steiner.

These results support the hypothesis that at least one hydrogen bond between H–O41–H and one chlorine ligand of the neighbor molecule of **3** exists in the crystal.

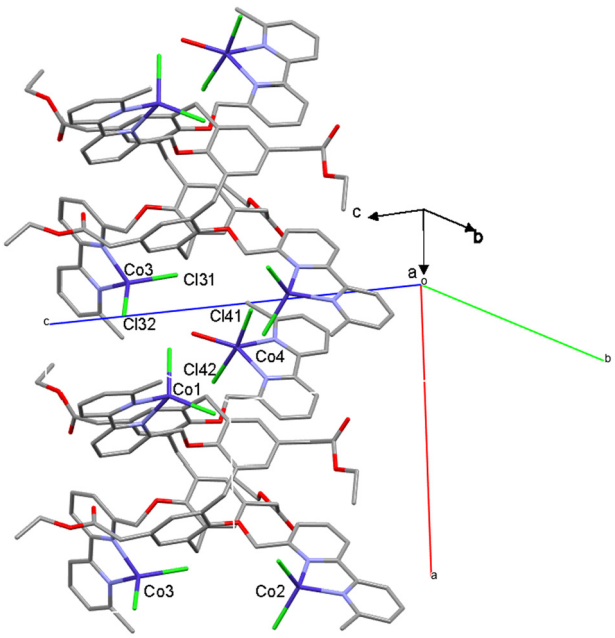

Fig. 12 Two molecules of complex **3** at 90 K in two adjacent unit cells, with a focus on the orientation of coordinating O41 atom in the penta-coordinated Co4 subunit towards the adjacent tetrahedral Co3 one.

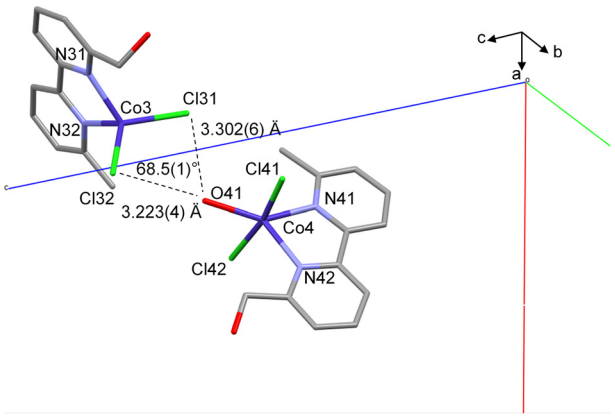

Fig. 13 Probable hydrogen bonding between two neighboring complex **3** molecules at the common border of two unit cells, involving the penta-coordinated Co4 entity and the tetrahedral one (Co3)′, at 90 K.

Table 5 Particular geometric parameters involving two hypothetical hydrogens **Ha** and **Hb** around **O41** between subunits **Co4** and **Co3′** of complex **3**. Evaluation of possible hydrogen bonds

Distances [Å]		Angles [°]	
O41–(Co3)′	3.906(5)	(Cl31)′–O41–(Cl32)′	68.5(1)
O41–(Cl31)′	3.302(6)	(Cl31)′–O41–(Co3)′	34.56(1)
O41–(Cl32)′	3.223(4)	(Cl32)′–O41–(Co3)′	34.64(6)
(Co3)′–(Cl31)′	2.217(2)	(Cl31)′–(Co3)′–(Cl32)′	111.63(7)
(Co3)′–(Cl32)′	2.220(2)		
O41–Ha	0.983[ad]	(Cl32)′–O41–Ha[b]	17.00[d]
O41–Hb	0.983[ad]	(Cl31)′–O41–Hb[b]	18.00[d]
(Cl32)′–Ha	2.30[cd]	(Cl32)′–Ha–O41[b]	157.00[d]
(Cl31)′–Hb	2.36[cd]	(Cl31)′–Hb–O41[b]	155.00[d]
Torsion angles [°]			
(Cl31)′–(Co3)′–(Cl32)′–O41	−14.3(1)		
O41–(Cl31)′–(Co3)′–(Cl32)′	14.0(1)		
(Cl32)′–O41–(Cl31)′–(Co3)′	−9.57(8)		
(Co3)′–(Cl31)′–O41–(Cl32)′	−9.57(8)		
(Co3)′–(Cl32)′–O41–(Cl31)′	9.55(8)		

[a] According to Steiner.[60] [b] Arbitrary positioning of Ha and Hb in the plane O41–(Cl31)′–(Co3)′–(Cl32)′. [c] Distances deduced from drawing (Fig. 14). [d] esd not available.

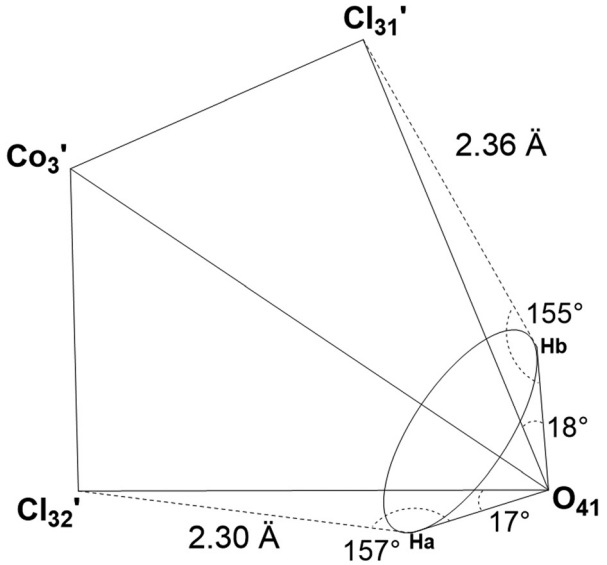

Fig. 14 Schematic representation of **Co4**/**Co3**′ subunit environment at the cell interface. Evaluation of possible hydrogen bonds involving the H_2O molecule bound to **Co4** and chlorine atoms bond to neighbor **Co3**′.

Experimental part

General

Chemistry. IRTF spectroscopy was performed in ATR mode on diamond crystal on a Shimadzu IRAffinity-1S spectrophotometer, at ambient temperature in the 400 to 4000 cm^{-1} wavenumber range. UV-Visible spectra were obtained between 2500 and 1000 nm using a UV MC2 apparatus (SAFAS, Monaco) with 110-QS Hellma quartz cells (10 mm light path, 3.5 mL capacity), λ_{max} in nm and ε in mol^{-1} dm^3 cm^{-1}. ^{1}H- and ^{13}C-NMR spectra were recorded on a Bruker AVANCE III 400 MHz (chemical shifts in ppm, J in Hz). Mass spectra (electrospray ionization – ESI) were recorded on a Bruker micrOTOFQ or a Xevo G2 XS Waters apparatus, at the Service Commun de Spectrométrie de Masse Organique, Nancy (MASSLOR).

Elemental analysis was performed on a Flash Smart (Thermofisher) apparatus at the Service de Microanalyse, Nancy (SYNBION). Merck TLC plates were used for chromatographic analysis (SiO_2, ref. 1.05554; Al_2O_3, ref. 1.05581). Separations by column chromatography were done on aluminium oxide 90 standardized Merck 1.01097 and silica gel 60 M Macherey-Nagel (0.04–0.063 mm). All commercially available products were used without further purification, unless otherwise specified.

Single-crystal studies. A single crystal of 0.2 × 0.2 × 0.4 mm (parallelepipedic shape) was glued onto the tip of a quartz fiber, and mounted on a goniometric head. Data acquisition was performed at 90 K using a Bruker APEX-II diffractometer equipped with a QAZAR CCD detector using Mo Kα radiation (λ = 0.71073 Å) at the Institut Jean Lamour of Nancy. Cell refinement and data reduction were carried out using the APEX2 Software.[62] The structure solution was obtained using direct methods, refined using full-matrix least-squares techniques with olex2-1.3[63] and refined with SHELXL-2018/3 software, implemented in the WinGX suite.[64]

NMR studies. NMR experiments were performed on a Bruker Avance III spectrometer operating at 9.4 Tesla (400 MHz and 100.6 MHz for ^{1}H and ^{13}C, respectively), using a Bruker 5 mm BBFO probe. Pulse widths were 15.6 ms for ^{1}H and 10.5 ms for ^{13}C. All experiments were performed at room temperature. Experiments were processed using the Bruker Topspin software package. For the paramagnetic cobalt complexes, the ^{1}H, ^{13}C decoupled from proton, ^{1}H–^{1}H DQF-COSY, ^{1}H–^{13}C HSQC NMR experiments were run with increased spectral width, given in the following section.

Acquisition parameters. 1D ^{1}H spectral width 60 kHz, 1D ^{13}C spectral width 40 kHz, and repetition time of 2 s.

Double quantum filtered COSY experiment. 4k complex points × 512 increments; 8 scans per increment; spectral width 60 kHz; the cardinal sine window function was used in both domains prior to Fourier transformations; final matrix size: 1k × 1k.

^{1}H–^{13}C HSQC experiment. 1k × 256 data set, 128 scans per increment; ^{1}H spectral width 80 kHz; ^{13}C spectral width 40 kHz; the cardinal sine window function was used in both domains prior to Fourier transformations; final matrix size: 1k × 1k.

Syntheses

5,11,17,23-Tetra(acetic acid)-25,26,27,28-tetrakis[(6′-methyl-2.2′-bipyridyl-6-yl)methoxy]calix[4]arene, 5,11,17,23-tetraethyl ester

2. K_2CO_3 (0.20 g, 1.43 × 10^{-3} mol) was added to a solution of 5,11,17,23-tetra(acetic acid)-calix[4]arene-25,26,27,28-tetrol, 5,11,17,23-tetraethyl ester **1**[37] (0.50 g, 0.65 × 10^{-3} mol) in dry MeCN (50 mL) under argon. The resulting suspension was stirred under reflux for 30 min. 6-Bromomethyl-6′-methyl-2,2′-bipyridine[38] (0.70 g, 2.66 × 10^{-3} mol) was then added, and reflux was continued under argon over 20 h (TLC monitoring: SiO_2, CH_2Cl_2, EtOH 3%). After cooling, the solvent was evaporated to dryness and the residue was dissolved in CH_2Cl_2. The inorganic insoluble material was filtered off and the filtrate was concentrated prior purification by column chromatography (Al_2O_3, CH_2Cl_2/hexane, 90 : 10) to give the ligand **2**. White powder. (0.37 g; 40%). IR (pure; ATR): 785.03 (strong, C═C–H with two C–H neighbors); 1033.84 (medium, C–O–C); 1147.64 (large, strong, C–O ester and ether); 1438.89 (strong, sharp, C═C–H deformations, CH_3 elongations); 1571.89 (strong, pyridyl C═N, C═C valence vibrations); 1730.15 (strong, COOEt); 2790–3145 (broad, C═C–H). UV-Vis (CH_2Cl_2): 292 (68224). ^{1}H-NMR (400 MHz, $CDCl_3$ (7.26 ppm), Fig. S5, ESI†): 1.10 (t, J = 7.1 Hz, 12 H, OCH_2CH_3), 2.70 (s, 12 H, CH_3 bpy), 2.74 (s, 8 H, CH_2COOEt), 3.75 (s, 8 H, $ArCH_2Ar$), 3.93 (q, J = 7.15 Hz, 8 H, OCH_2CH_3), 4.96 (s, 8 H, OCH_2bpy), 6.67 (s, 8 H, Ar*H*), 6.75 (d, J = 7.5 Hz, 4 H, Ar*H* bpy), 7.21 (d, J = 7.5 Hz, 4 H, Ar*H* bpy), 7.75 (t, J = 7.7 Hz, 8 H, Ar*H* bpy), 8.28 (d, J = 7.8 Hz, 4 H, Ar*H* bpy), 8.48 (d, J = 7.6 Hz, 4 H, Ar*H* bpy). ^{13}C-NMR (100 MHz, $CDCl_3$ (77.0 ppm)): 14.08 (OCH_2CH_3), 24.62 (CH_3 bpy), 37.45 ($ArCH_2Ar$), 40.20 (CH_2COOEt), 60.53 (OCH_2CH_3), 72.70 (OCH_2bpy), 118.35, 119.59, 121.53, 123.50 (C_3, $C_{3'}$, C_5, $C_{5'}$), 128.02 (C_p), 131.26 (C_m), 134.12 (C_o), 136.91, 137.39, 153.96, 154.72, 155.20, 157.29, 157.91 (C_2, $C_{2'}$, C_4, $C_{4'}$, C_6, $C_{6'}$, C_{ipso}),

171.69 (*C*O). Anal. calc. for $C_{92}H_{88}O_{12}N_8$ (1497.73): C 73.78, H 5.92, N 7.48; found: C 74.21, H 5.93, N 7.50. Positive mode ESI-MS: 1498.66 $[M + H^+]^+$, 1314.57 $[M - C_{12}H_{11}N_2 + H^+]^+$, 1131.48 $[M - 2\ C_{12}H_{11}N_2 + H^+]^+$, 948.38 $[M - 3\ C_{12}H_{11}N_2 + H^+]^+$, 749.33 $[M + 2\ H^+]^{2+/2}$, 500.22 $[M + 3\ H^+]^{3+/3}$.

5,11,17,23-Tetra(acetic acid)-25,26,27,28-tetrakis[(6′-methyl-2.2′-bipyridyl-6-yl)methoxy]calix[4]arene, 5,11,17,23-tetraethyl ester, tetra (dichlorocobalt(II)) complex

3. An ultramarine blue solution of $CoCl_2{\cdot}6H_2O$ (105.5×10^{-3} g; 4.433×10^{-4} mol; 4.0 equiv.) in EtOH (2.0 mL) was added to a stirred solution of ligand **2** (166.0×10^{-3} g, 1.108×10^{-4} mol) in CH_2Cl_2 (12 mL) under Ar, to give a blue solution at *ca.* 11% of EtOH after rinsing with CH_2Cl_2 (4 mL). After 2 minutes of stirring, the solution became cloudy with a nice blue moiré-effect. Stirring was continued under Ar for 16 h, and the solvents were then evaporated to dryness. The resulting solid was treated with CH_2Cl_2 and the insoluble blue material was recovered by filtration on a crucible (0.188 g after drying under vacuum, 82%). The blue filtrate was then evaporated to dryness (0.035 g), in accordance with a quantitative yield. IR (pure, ATR): 785.03 (medium, C═C–H), 1143.79 (m, C–O ester and ether), 1598.98 (C═N), 1716.64 (m, COOEt). UV-Vis (CH_2Cl_2): 317 (44 356), 343 (sh, 21 312), 569 (985), 658 (1775). ^{1}H-NMR (400 MHz, CD_3CN (1.96 ppm) + CD_2Cl_2 (5.42 ppm), −90 to +120 ppm)): −44.92 (br s, $\Delta\nu_{\frac{1}{2}}$ = 407 Hz, 8 H, OC*H*$_2$bpy); −22.89 (br s, $\Delta\nu_{\frac{1}{2}}$ = 246 Hz, 12 H, C*H*$_3$bpy); −19.18 (br s, $\Delta\nu_{\frac{1}{2}}$ = 31 Hz, 4 H, Hpy b); −15.01 (br s, $\Delta\nu_{\frac{1}{2}}$ = 25 Hz, 4 H, Hpy a); −8.43 (br s, $\Delta\nu_{\frac{1}{2}}$ = 50 Hz, 8 H), −3.73 (br s, $\Delta\nu_{\frac{1}{2}}$ = 38 Hz, 8 H), −1.33 (br s, $\Delta\nu_{\frac{1}{2}}$ = 14 Hz, 8 H, C*H*$_2$COOEt; 4.27 (br s, $\Delta\nu_{\frac{1}{2}}$ = 17 Hz, 12 H, OCH$_2$C*H*$_3$); 7.36 (br s, $\Delta\nu_{\frac{1}{2}}$ = 22 Hz, 8 H, OC*H*$_2$CH$_3$); 31.96 (br s, $\Delta\nu_{\frac{1}{2}}$ = 35 Hz, 4 H, Hpy b); 53.81 (br s, $\Delta\nu_{\frac{1}{2}}$ = 25 Hz, 4 H, Hpy a); 67.16 (br s, $\Delta\nu_{\frac{1}{2}}$ = 28 Hz, 4 H, Hpy b); 74.07 (br s, 4 H, $\Delta\nu_{\frac{1}{2}}$ = 25 Hz, 4 H, Hpy a). ^{13}C-NMR (partial resolution, HSQC; −40 to +800 ppm; CD_3CN (1.972/1.32 + 118.26 ppm) + CD_2Cl_2 (5.412/55.11 ppm)): 19.03 (coupled to ^{1}H 4.27; OCH$_2$C*H*$_3$); 38.84 (coupled to ^{1}H −1.32; C*H*$_2$COOEt); 64.51 (coupled to ^{1}H 7.36, OC*H*$_2$CH$_3$); 120.37 (coupled to ^{1}H −3.73, *Ar*H); ^{13}C-NMR (CD_3CN (1.32 + 117.45 ppm) + $CDCl_3$ (78.57 ppm): 19.08 (*q*, J_{H-C} = 126 Hz, $\Delta\nu_{\frac{1}{2}}$ = 12 Hz, OCH$_2$C*H*$_3$ from HSQC); 27.96 (t, J_{H-C} = 125 Hz, $\Delta\nu_{\frac{1}{2}}$ = 19 Hz, Ar–C*H*$_2$–Ar); 38.63 (t, J_{H-C} = 129 Hz, $\Delta\nu_{\frac{1}{2}}$ = 12 Hz, C*H*$_2$COOCH$_2$CH$_3$); 63.80 (t, J_{H-C} = 145 Hz, $\Delta\nu_{\frac{1}{2}}$ = 12 Hz, OC*H*$_2$CH$_3$ from HSQC); 81.88 (s, $\Delta\nu_{\frac{1}{2}}$ = 30 Hz, C_{quat}); 119.26 (s, $\Delta\nu_{\frac{1}{2}}$ = 12 Hz, $C_{ipso,ortho,para}$ of Ar); 119.63 (d, *J* = 157 Hz, $\Delta\nu_{\frac{1}{2}}$ = 24 Hz, *C*H of Ar); 134.49 (s, $\Delta\nu_{\frac{1}{2}}$ = 14 Hz, $C_{ipso,ortho,para}$ of Ar); 171.17 (s, $\Delta\nu_{\frac{1}{2}}$ = 14 Hz, $C_{ipso,ortho,para}$ of Ar); 183.20 (s, $\Delta\nu_{\frac{1}{2}}$ = 38 Hz, C(O)); 263.16 (d, J_{H-C} = 165 Hz, $\Delta\nu_{\frac{1}{2}}$ = 22 Hz, *C*H of bpy); 297.52 (d, J_{H-C} = 165 Hz, $\Delta\nu_{\frac{1}{2}}$ = 22 Hz, *C*H of bpy); 319.22 (d, J_{H-C} = 165 Hz, $\Delta\nu_{\frac{1}{2}}$ = 22 Hz, *C*H of bpy); 321.60 (d, J_{H-C} = 165 Hz, $\Delta\nu_{\frac{1}{2}}$ = 17 Hz, *C*H of bpy); 331.31 (s, $\Delta\nu_{\frac{1}{2}}$ = 40 Hz, $C_{2,2',6,6'}$ of bpy); 375.33 (s, $\Delta\nu_{\frac{1}{2}}$ = 40 Hz, $C_{2,2',6,6'}$ of bpy); 404.90 (br s, $C_{2,2',6,6'}$ of bpy); 428.00 (br s, $C_{2,2',6,6'}$ of bpy); 457.16 (d, J_{H-C} = 173 Hz, $\Delta\nu_{\frac{1}{2}}$ = 28 Hz, *C*H of bpy); 480.63 (d, J_{H-C} = 173 Hz, $\Delta\nu_{\frac{1}{2}}$ = 28 Hz, *C*H of bpy). Anal. calc. for $C_{92}H_{88}Cl_8Co_4N_8O_{12}$, 3 H_2O (2071.14; powder before crystallization): C 53.35, H 4.57, N 5.41, O 11.59; found: C 53.03, H 4.37, N 5.37, O 11.31. Positive mode ESI-MS (Fig. S6 and S7, ESI†): 1535.92, 1536.92, 1537.92, 1538.92 $[M - 4\ (CoCl_2) + K^+]^+$; 1519.95, 1520.95 $[M - 4\ (CoCl_2) + Na^+]^+$; 1496.98, 1497.98 $[M - 4\ (CoCl_2) + H^+]^+$; 1131.48, 1132.49, 1133.48, 1134.47 $[M - 4\ (CoCl_2) - 2(CH_3bpyCH_2) + H^+]^+$; 1017.75, 1018.42, 1018.75, 1019.09 $[2\ L + Co^{2+} + H^+]^{3+/3}$; 880.70, 881.20, 881.70, 882.20, 882.70, 883.20, 883.70, 884.21, 884.71, 885.19, 885.71 $[M - 2\ (CoCl_2) + Li + H^+]^{2+/2}$; 813.77, 814.28, 814.77, 815.28, 815.79, 816.27, 816.78, 817.27, 817.77, 818.28, 818.77, 819.27, 819.77 $[M - 3\ (CoCl_2) - Cl^- + K^+]^{2+/2}$; 798.79, 799.28, 799.79, 800.29, 800.79, 801.30, 801.80, 802.30 $[M - 3\ (CoCl_2) - Cl^- + Li^+]^{2+/2}$; 795.79, 796.28, 796.78 $[M - 3\ (CoCl_2) - Cl^- + H^+]^{2+/2}$.

(6′6′-Dimethyl-2,2′-bipyridyl)Co(Cl)$_2$; dmbp(CoCl$_2$)

4. An ultramarine blue solution of $CoCl_2{\cdot}6H_2O$ (0.272 g, 1.05 equiv.) in CH_3OH (5 mL) was added dropwise to a solution of 6′,6′-dimethyl-2,2′-bipyridine (0.2 g, 1.085×10^{-3} mole) in $CHCl_3$ (10 mL). This resulted in a quasi-immediate precipitation of a blue microcrystalline solid. The mixture was stirred under argon for two days and the precipitate was filtered off, rinsed with $CHCl_3$ and then Et_2O to afford the deep-blue green microcrystalline complex **4** (0.32 g; 94%) after drying under high vacuum. IR (pure, ATR): 792.74 (strong, C═C–H), 1560.20 (C═C), 1598.99 (C═N). UV-Vis (CH_2Cl_2): 316 (10 168), 339 (5780), 571 (263), 654 (530). ^{1}H-NMR ($CDCl_3$ (7.26 ppm)): −21.64 (br s, 6 H, $\Delta\nu_{\frac{1}{2}}$ = 145 Hz, C*H*$_3$bpy), −15.03 (s, 2 H, $\Delta\nu_{\frac{1}{2}}$ = 18 Hz, *H*(3) or *H*(4) or *H*(5) bpy), 47.23 (s, 2 H, $\Delta\nu_{\frac{1}{2}}$ = 19 Hz, *H*(3) or *H*(4) or *H*(5) bpy), 69.75 (2 H, $\Delta\nu_{\frac{1}{2}}$ = 19 Hz, *H*(3) or *H*(4) or *H*(5) bpy). ^{1}H-NMR (CD_3OD 3.34 ppm + $CDCl_3$ 7.26 ppm; −80 to +120 ppm): −35.20 (br s, 6 H, $\Delta\nu_{\frac{1}{2}}$ = 770 Hz, C*H*$_3$bpy), −9.95 (br s, 2 H, $\Delta\nu_{\frac{1}{2}}$ = 130 Hz, *H*(3) or *H*(4) or *H*(5) bpy), 48.89 (br s, 2 H, $\Delta\nu_{\frac{1}{2}}$ = 70 Hz, *H*(3) or *H*(4) or *H*(5) bpy), 73.17 (br s, 2 H, $\Delta\nu_{\frac{1}{2}}$ = 80 Hz, *H*(3) or *H*(4) or *H*(5) bpy). ^{13}C-NMR ((H)DMF): 33.74 (q, J_{H-C} = 138 Hz, *C*H$_3$ of DMF); 39.11 (q, J_{H-C} = 138 Hz, *C*H$_3$ of DMF); 165.85 (d, J_{H-C} = 192 Hz, H*C*(O) of DMF); 139.78 (br s, $\Delta\nu_{\frac{1}{2}}$ = 40 Hz, *C*H$_3$ of bpy); 295.13 (d, J_{H-C} = 170 Hz, $\Delta\nu_{\frac{1}{2}}$ = 50 Hz, H*C* of pyr); 313.24 (d, J_{H-C} = 170 Hz, $\Delta\nu_{\frac{1}{2}}$ = 16 Hz, H*C* of pyr); 348.00 (br s, $\Delta\nu_{\frac{1}{2}}$ = 400 Hz, C_{quat} of pyr); 362.00 (br s, $\Delta\nu_{\frac{1}{2}}$ = 240 Hz, C_{quat} of pyr); 475.20 (d, J_{H-C} = 170 Hz, $\Delta\nu_{\frac{1}{2}}$ = 77 Hz, H*C* of pyr). Anal. calc. for $C_{12}H_{12}Cl_2CoN_2$ (314.075): C 45.89, H 3.85, N 8.92; found: C 46.00, H 3.90, N 8.92.

Crystallisation conditions

*Complex **3***. Deep-blue crystals suitable for X-ray diffraction analysis were obtained after some days in a vial equipped with a hood in polypropylene crossed by an injection needle, by slow evaporation of CH_2Cl_2 from a solution of complex **3** in MeCN (*ca.* 10 mg for 12 mL) and CH_2Cl_2. Crystals were maintained in the mother liquor to avoid irreversible and deleterious desiccation.

Conclusions

A new calixarene ligand incorporating four ethylacetate groups at the ''upper'' rim and four dimethyl bipyridines at the ''lower'' rim was obtained surprisingly in the 1,3-alternate conformation, hence generating an interesting tube-like ligand that presents multi-chelating behavior for transition metal ions adopting the tetrahedral coordination geometry. Its neutral, blue, paramagnetic complex with $CoCl_2$ has been prepared and characterized with UV-visible spectroscopy and NMR in solution, and by X-ray diffraction study in the solid state.

In solution, it showed the expected capacity of complexation of 4 cobalt units per calixarene by UV-vis titration. 1D- and COSY-^{1}H-NMR operated between −50 and +80 ppm confirmed its paramagnetism, and showed its high symmetry with a unique bipyridyl resonance signal system. Its ^{13}C-NMR spectrum was recorded over a window from 700 to −100 ppm, affording interesting results in terms of chemical shifts and structure elucidation for such paramagnetic complexes. The resulting predicted model structure involving four bipyridyl($CoCl_2$) subunits, in which Co(II) is coordinated in tetrahedral geometry by two bipyridyl N atoms and two chlorine ions, organized in 1,3-alternate conformation was partially confirmed in the solid state by X-ray diffraction analysis. In fact, one of the four bipyridyl($CoCl_2$) subunits, at the unit cell border and close to a nearby cell bipyridyl($CoCl_2$) unit incorporates an oxygen atom as the fifth ligand, generating a pentacoordinated cobalt complex in distorted trigonal bipyramid geometry with the two Cl at the apex, and the two N and O in the base triangle. The cobaltous status was postulated based on the bipyridyl N–Co distances of *ca.* 2.07 Å, indicating the neutral status of the oxygen and, by this way, its aqueous nature. This H_2O molecule was finally described as a H-bond linker with one or two chlorine ligands of the tetrahedral bipyridyl($CoCl_2$) subunit of the neighbor cell, participating by its presence in the crystallization or stabilization. Further magnetism and electrochemistry studies of this paramagnetic species are underway.

Data availability

The data supporting this article NJ-ART-05-2024-002476 "Synthesis of tube-like tetra-bipyridyl, tetra-ethylacetato-calix[4]arene in 1,3-alternate conformation and the unexpected crystal structure of its [bpy($CoCl_2$)]$_3$-[bpy($CoCl_2$)(H_2O)] complex" proposed by Regnouf de Vains Jean-Bernard have been included as part of the ESI.†

Conflicts of interest

There are no conflicts to declare.

Acknowledgements

We thank the Ministère de l'Enseignement Supérieur et de la Recherche, the CNRS and the Région Lorraine for financial support. S. Adach from Service Central d'Analyse Elémentaire, Université de Lorraine and F. Dupire from Plateforme de Spectrométrie de Masse de l'Université de Lorraine are acknowledged for elemental analysis and mass spectrometry respectively, as well as M. Zimmermann for his technical assistance during initial complexation studies. We thank Prof. S. Bouguet-Bonnet, from CRM2 laboratory for fruitful discussions on NMR, and Dr M. Bouché from L2CM for her assistance in manuscript revision and corrections.

Notes and references

1 C. D. Gutsche, in *Syntheses of macrocycles, the design of selective complexing agents, Progress in Macrocyclic Chemistry*, ed. R. M. Izatt and J. J. Christensen, John Wiley and Sons, New York, 1987, vol. 3. pp. 93–166.
2 C. D. Gutsche, in *"Calixarenes", Monographs in Supramolecular Chemistry*, ed. J. F. Stoddart, Royal Society of Chemistry, Cambridge, 1989.
3 *Calixarenes. A Versatile Class of Macrocyclic Compounds*, ed. J. Vicens and V. Böhmer, Kluwer Academic Publishers, Dordrecht, 1991.
4 *Calixarenes in the nanoworld*, ed. J. Vicens, J. Harrowfield and L. Baklouti, Kluwer, Dordrecht, The Netherlands, 2007.
5 C. D. Gutsche, *Calixarenes Revisited*, Royal Society of Chemistry, Cambridge, 1998.
6 *Calixarenes 2001*, ed. Z. Asfari, V. Böhmer, J. Harrowfield and J. Vicens, Kluwer, Dordrecht, The Netherlands, 2001.
7 C. Wieser, C. B. Dieleman and D. Matt, *Coord. Chem. Rev.*, 1997, **165**, 93–161.
8 *Calixarenes for separations*, ed. L. G. Lumetta, R. D. Rogers and A. S. Gopalan, ACS Symposiums Series 757, American Chemical Society, 2000.
9 Ref. 6, chapters 19, 20, 21, 22, 27 and 28.
10 R. Ludwig, *Fresenius' J. Anal. Chem.*, 2000, **367**, 103–128.
11 W. Sliwa and M. Deska, *ARKIVOC*, 2008, **i**, 87–127.
12 W. Sliwa and T. Girek, *J. Inclusion Phenom. Macrocyclic Chem.*, 2010, **66**, 15–41.
13 W. Sliwa, *J. Inclusion Phenom. Macrocyclic Chem.*, 2005, **52**, 13–37.
14 B. Mokhtari and K. Pourabdollah, *Asian J. Chem.*, 2013, **25**, 1–12.
15 M. Deska, B. Dondela and W. Sliwa, *ARKIVOC*, 2015, 393–416.
16 N. Kotzen and A. Vigalok, *Supramol. Chem.*, 2008, **20**, 129–139.
17 J. Konczyk, A. Nowik-Zajac and C. A. Kozlowski, *Sep. Sci. Technol.*, 2016, **51**, 2394–2410.
18 B. Mokhtari and K. Pourabdollah, *Asian J. Chem.*, 2011, **23**(11), 4717–4734.
19 For example: J.-N. Rebilly and O. Reinaud, *Supramol. Chem.*, 2014, **26**, 454–479.
20 J.-B. Regnouf-de-Vains and R. Lamartine, *Helv. Chim.Acta*, 1994, 77, 1817–1825.
21 J.-B. Regnouf-de-Vains, S. Pellet-Rostaing and R. Lamartine, *Tetrahedron Lett.*, 1995, **36**, 5745–5748.
22 J.-B. Regnouf-de-Vains, R. Lamartine, B. Fenet, C. Bavoux, A. Thozet and M. Perrin, *Helv. Chim. Acta*, 1995, **78**, 1607–1619.
23 S. Pellet-Rostaing, J.-B. Regnouf-de-Vains, R. Lamartine, P. Meallier, S. Guittonneau and B. Fenet, *Helv. Chim. Acta*, 1997, **80**, 1229–1243.
24 J.-B. Regnouf-de-Vains, R. Lamartine and B. Fenet, *Helv. Chim. Acta*, 1998, **81**, 661–669.
25 S. Pellet-Rostaing, J.-B. Regnouf-de-Vains, R. Lamartine and B. Fenet, *Inorg. Chem. Commun.*, 1999, **2**, 4–7.
26 Y. Molard, C. Bureau, H. Parrot-Lopez, R. Lamartine and J.-B. Regnouf-de-Vains, *Tetrahedron Lett.*, 1999, **40**, 6383–6387.
27 J.-O. Dalbavie, J.-B. Regnouf-de-Vains, R. Lamartine, S. Lecocq and M. Perrin, *Eur. J. Inorg. Chem.*, 2000, 683–691.

28 J.-B. Regnouf-de-Vains, J.-O. Dalbavie, R. Lamartine and B. Fenet, *Tetrahedron Lett.*, 2001, **42**, 2681–2684.
29 J.-O. Dalbavie, J.-B. Regnouf-de-Vains, R. Lamartine, M. Perrin, S. Lecocq and B. Fenet, *Eur. J. Inorg. Chem.*, 2002, 901–909.
30 P. Engrand and J.-B. Regnouf-de-Vains, *Tetrahedron Lett.*, 2002, **43**, 8863–8866.
31 N. Psychogios, J.-B. Regnouf-de-Vains and H. Stoeckli-Evans, *Eur. J. Inorg. Chem.*, 2004, 2514–2523.
32 Y. de Gaetano, I. Clarot and J.-B. Regnouf-de-Vains, *Tetrahedron Lett.*, 2009, **42**, 5793–5797.
33 B. Korchowiec, M. Orlof, G. Sautrey, A. Ben Salem, J. Korchowiec, J.-B. Regnouf de Vains and E. Rogalska, *J. Phys. Chem. B*, 2010, **114**, 10427–10435.
34 Y. De Gaetano, I. Clarot and J.-B. Regnouf-de-Vains, *New J. Chem.*, 2012, **36**, 1339–1346.
35 J.-B. Regnouf-de-Vains, B. Malaman, S. Bouguet-Bonnet, S. Poinsignon, S. Leclerc and M. Beley, *New J. Chem.*, 2019, **43**, 13282–13293.
36 G. R. Newkome, D. C. Pantaleo, W. E. Puckett, P. L. Ziefle and W. A. Deutsch, *J. Inorg. Nucl. Chem.*, 1981, **43**, 1529–1531.
37 M. Mourer, N. Psychogios, G. Laumond, A.-M. Aubertin and J.-B. Regnouf-de-Vains, *Bioorg. Med. Chem.*, 2010, **18**, 36–45.
38 J.-C. Rodriguez-Ubis, B. Alpha, D. Plancherel and J.-M. Lehn, *Helv. Chim. Acta*, 1984, **64**, 2264–2269.
39 S. K. Sharma and C. D. Gutsche, *Tetrahedron Lett.*, 1993, **34**, 5389–5392.
40 S. K. Sharma and C. D. Gutsche, *Tetrahedron*, 1994, **50**, 4087–4104.
41 L. Banci, A. Bencini, C. Benelli, D. Gatteschi and C. Zanchini, *Struct. Bond.*, 1982, **52**, 37–86, chapter 2, in: Structures *versus* Special Properties; Conferences Proceedings, Springer Verlag, Heidelberg.
42 I. Bertini, in *Coordination Chemistry of Metalloenzymes, NATO Advanced Study Institutes Series, Series C: Mathematical and Physical Sciences*, ed. I. Bertini, R. S. Drago and C. Luchinat, D. Reidel Publishing Company, Dordrecht, Boston and London, 1983, pp. 1–18.
43 C. Sartorius, M. F. Dunn and M. Zappezauer, *Eur. J. Biochem.*, 1988, **177**, 493–499.
44 V. K. Voronov, I. A. Ushakov and E. A. Funtikova, *Heliyon*, 2022, **8**, e09202.
45 G. L. Baker, F. R. Fronczek, G. E. Kiefer, C. R. Marston, C. L. Modenbach, G. R. Newkome, W. E. Puckett and S. F. Watkins, *Acta Crystallogr., Sect. C: Cryst. Struct. Commun.*, 1988, **44**, 1668–1669.
46 N. A. Torbati, A. R. Rezvani, N. Safari, H. Saravania and V. Amanib, *Acta Crystallogr., Sect. E: Struct. Rep. Online*, 2010, **66**, m1284.
47 D. N. Tran, PhD Thesis report, Université de Lorraine, 2008, pp. 129, 145, 187.
48 B. Brewer, N. R. Brooks, S. Abdul-Halim and A. G. Sykes, *J. Chem. Crystallogr.*, 2003, **33**, 651–662.
49 M. Gennari, B. Gerey, N. Hall, J. Pécaut, M.-N. Collomb, M. Rouzières, R. Clérac, M. Orio and C. Duboc, *Angew. Chem., Int. Ed.*, 2014, **53**, 5318–5321.
50 D. Brazzolotto, M. Gennari, S. Yu, J. Pécaut, M. Rouzières, R. Clérac, M. Orio and C. Duboc, *Chem. – Eur. J.*, 2016, **22**, 925–933.
51 F. C. Kennedy, H. A. Hill, T. A. Kaden and B. L. Vallee, *Biochem. Biophys. Res. Commun.*, 1972, **48**, 1533–1539.
52 C. M. Harris, T. N. Lockyer and N. C. Stephenson, *Aust. J. Chem.*, 1966, **19**, 1741–1743.
53 E. Goldschmied and N. C. Stephenson, *Acta Crystallogr., Sect. B: Struct. Crystallogr. Cryst. Chem.*, 1970, **26**, 1867–1875.
54 **https://www.knowledgedoor.com/2/elements_handbook/shannon-prewitt_effective_ionic_radius.html**.
55 P. Comba, M. Kerscher, G. A. Lawrance, B. Martin, H. Wadepohl and S. Wunderlich, *Angew. Chem., Int. Ed.*, 2008, **47**, 4740–4743.
56 C. W. Reimann, M. Zocchi, A. D. Mighell and A. Santoro, *Acta Crystallogr., Sect. B: Struct. Crystallogr. Cryst. Chem.*, 1974, **27**, 2211–2218.
57 V. Thamilarasan, N. Sengottuvelan, A. Sudha, P. Srinivasan and G. Chakkaravarthi, *J. Photochem. Photobiol., B*, 2016, **162**, 558–569.
58 S. Arora, D. Talwar, M. Chetal, V. K. Bhardwaj, A. Dawar, H. Sidhu, S. Kashyap and N. Capalash, *J. Mol. Struct.*, 2022, **1247**, 131279.
59 M. Toyama, Y. Yamamoto, T. Yoshimoto and K. Katagiri, *J. Mol. Struct.*, 2021, **1244**, 130938.
60 T. Steiner, *Acta Crystallogr., Sect. B: Struct. Sci.*, 1998, **54**, 456–463.
61 I. Pethes, I. Bakó and L. Pusztai, *Phys. Chem. Chem. Phys.*, 2020, **22**, 11038–11044.
62 *T M86-E01078APEX2 User Manual*, Bruker AXS Inc., Madison, USA, 2006.
63 O. V. Dolomanov, L. J. Bourhis, R. J. Gildea, J. A. K. Howard and H. Puschmann, *J. Appl. Crystallogr.*, 2009, **42**, 339–341.
64 X. L. J. Farrugia, *J. Appl. Crystallogr.*, 2012, **45**, 849–854.